Ab initio calculations of $BaTiO_3$ and $PbTiO_3$ (001) and (011) surface structures

R. I. Eglitis and David Vanderbilt
Department of Physics and Astronomy, Rutgers University, 136 Frelinghuysen Road, Piscataway, New Jersey 08854-8019, USA
(Received 3 October 2007; published 31 October 2007)

We present and discuss the results of calculations of surface relaxations and rumplings for the (001) and (011) surfaces of $BaTiO_3$ and $PbTiO_3$ using a hybrid B3PW description of exchange and correlation. On the (001) surfaces, we consider both AO (A=Ba or Pb) and TiO_2 terminations. In the former case, the surface AO layer is found to relax inward for both materials, while outward relaxations of all atoms in the second layer are found at both kinds of (001) terminations and for both materials. The surface relaxation energies of BaO and TiO_2 terminations on $BaTiO_3$ (001) are found to be comparable, as are those of PbO and TiO_2 on $PbTiO_3$ (001), although in both cases the relaxation energy is slightly larger for the TiO_2 termination. As for the (011) surfaces, we consider three types of surfaces, terminating on a TiO layer, a Ba or Pb layer, or an O layer. Here, the relaxation energies are much larger for the TiO-terminated surface than for the Ba- or Pb-terminated surfaces. The relaxed surface energy for the O-terminated surface is about the same as the corresponding average of the TiO- and Pb-terminated surfaces on $PbTiO_3$, but much less than the average of the TiO- and Ba-terminated surfaces on $BaTiO_3$. We predict a considerable increase of the Ti-O chemical bond covalency near the $BaTiO_3$ and $PbTiO_3$ (011) surfaces as compared to both the bulk and the (001) surface.

DOI: 10.1103/PhysRevB.76.155439 PACS number(s): 68.35.Ct, 68.35.Md, 68.47.Gh

I. INTRODUCTION

Thin films of ABO_3 perovskite ferroelectrics play an important role in numerous microelectronic, catalytic, and other high-technology applications, and are frequently used as substrates for growth of other materials such as cuprate superconductors.[1,2] Therefore, it is not surprising that a large number of *ab initio* quantum-mechanical calculations,[3–13] as well as several classical shell-model (SM) studies,[14–16] have dealt with the atomic and electronic structures of the (001) surface of $BaTiO_3$, $PbTiO_3$, and $SrTiO_3$ crystals. In order to study the dependence of the surface relaxation properties on the exchange-correlation functionals and the type of basis (localized vs plane wave) used in the calculations, a detailed comparative study of $SrTiO_3$ (001) surfaces based on ten different quantum-mechanical techniques[17,18] was recently performed.

Due to intensive development and progressive miniaturization of electronic devices, the surface structure as well as the electronic properties of the ABO_3 perovskite thin films have been extensively studied experimentally in recent years. The $SrTiO_3$ (001) surface structure has been analyzed by means of low-energy electron diffraction (LEED),[19] reflection high-energy electron diffraction (RHEED),[20] x-ray photoelectron spectroscopy (XPS), ultraviolet electron spectroscopy, medium-energy ion scattering,[21] and surface x-ray diffraction.[22] Nevertheless, it is important to note that the LEED[19] and RHEED[20] experiments contradict each other in the sign (contraction or expansion) of the interplanar distance between the top metal atom and the second crystal layer for the SrO-terminated $SrTiO_3$ (001) surface. The most recent experimental studies on the $SrTiO_3$ surfaces include a combination of XPS, LEED, and time-of-flight scattering and recoil spectrometry (TOF-SARS),[23] as well as metastable impact electron spectroscopy.[24] In these recent studies, well-resolved 1×1 LEED patterns were obtained for the TiO_2-terminated $SrTiO_3$ (001) surface. Simulations of the TOF-SARS azimuthal scans indicate that the O atoms are situated 0.1 Å above the Ti layer (surface plane) in the case of the TiO_2-terminated $SrTiO_3$ (001) surface.

While the (001) surfaces of $SrTiO_3$, $BaTiO_3$, and $PbTiO_3$ have been extensively studied, much less is known about the (011) surfaces. The scarcity of information about these surfaces is likely due to the polar character of the (011) orientation. (011) terminations of $SrTiO_3$ have frequently been observed, but efforts toward the precise characterization of their atomic-scale structure and corresponding electronic properties have only begun in the past decade, specifically using atomic-force microscopy,[25] scanning tunneling microscopy, Auger spectroscopy, and LEED[26] methods.

To the best of our knowledge, very few *ab initio* studies of perovskite (011) surfaces exist. The first *ab initio* study of the electronic and atomic structures of several (1×1) terminations of the (011) polar orientation of the $SrTiO_3$ surface was performed by Bottin *et al.*[27] One year later, Heifets *et al.*[28] performed very comprehensive *ab initio* Hartree-Fock calculations for four possible terminations (TiO, Sr, and two kinds of O terminations) of the $SrTiO_3$ (011) surface. Recently, Heifets *et al.*[29] performed *ab initio* density-functional calculations of the atomic structure and charge redistribution for different terminations of the $BaZrO_3$ (011) surfaces. However, despite the high technological potential of $BaTiO_3$ and $PbTiO_3$, we are unaware of any previous *ab initio* calculations performed for the $BaTiO_3$ and $PbTiO_3$ (011) surfaces. In this study, therefore, we have investigated the (011) as well as the (001) surfaces of $BaTiO_3$ and $PbTiO_3$, with an emphasis on the effect of the surface relaxation and rumpling, surface energies, and the charge redistributions and changes in bond strength that occur at the surface.

II. PRELIMINARIES

A. Computational method

We carry out first-principles calculations in the framework of density-functional theory (DFT) using the CRYSTAL com-

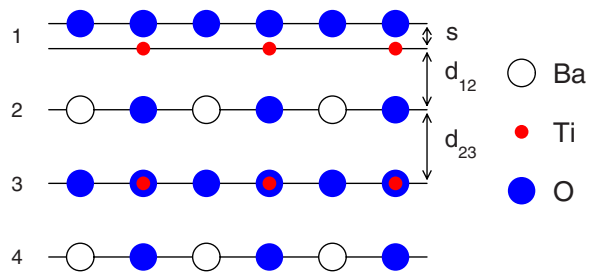

FIG. 1. (Color online) Side view of a TiO_2-terminated $BaTiO_3$ (001) surface with the definitions of the surface rumpling s and the near-surface interplanar distances d_{12} and d_{23}, respectively.

puter code.[30] Unlike the plane-wave codes employed in many previous studies,[31,32] CRYSTAL uses localized Gaussian-type basis sets. In our calculations, we adopted the basis sets developed for $BaTiO_3$ and $PbTiO_3$ in Ref. 33. Our calculations were performed using the hybrid exchange-correlation B3PW functional involving a mixture of nonlocal Fock exact exchange, local-density approximation (LDA) exchange, and Becke's gradient corrected exchange functional,[34] combined with the nonlocal gradient corrected correlation potential of Perdew and Wang.[35–37] We chose the hybrid B3PW functional for our current study because it yields excellent results for the $SrTiO_3$, $BaTiO_3$, and $PbTiO_3$ bulk lattice constant and bulk modulus.[17,33]

The reciprocal-space integration was performed by sampling the Brillouin zone with an $8\times8\times8$ Pack-Monkhorst mesh,[38] which provides a balanced summation in direct and reciprocal spaces. To achieve high accuracy, large enough tolerances of 7, 8, 7, 7, and 14 were chosen for the dimensionless Coulomb overlap, Coulomb penetration, exchange overlap, first exchange pseudo-overlap, and second exchange pseudo-overlap parameters, respectively.[30]

An advantage of the CRYSTAL code is that it treats isolated two-dimensional slabs, without any artificial periodicity in the z direction perpendicular to the surface, as commonly employed in most previous surface band-structure calculations (e.g., Ref. 8). In the present *ab initio* investigation, we have studied several isolated periodic two-dimensional slabs of cubic $BaTiO_3$ and $PbTiO_3$ crystals containing seven planes of atoms.

B. Surface geometries

The $BaTiO_3$ and $PbTiO_3$ (001) surfaces were modeled using symmetric (with respect to the mirror plane) slabs consisting of seven alternating TiO_2 and BaO or PbO layers, respectively. One of these slabs was terminated by BaO planes for the $BaTiO_3$ crystal (or PbO planes for $PbTiO_3$) and consisted of a supercell containing 17 atoms. The second slab was terminated by TiO_2 planes for both materials and consisted of a supercell containing 18 atoms. These slabs are nonstoichiometric, with unit cell formulas $Ba_4Ti_3O_{10}$ or $Pb_4Ti_3O_{10}$, and $Ba_3Ti_4O_{11}$ or $Pb_3Ti_4O_{11}$ for $BaTiO_3$ and $PbTiO_3$ perovskites, respectively. These two (BaO or PbO and TiO_2) terminations are the only two possible flat and dense (001) surfaces for the $BaTiO_3$ or $PbTiO_3$ perovskite lattice structure. The sequence of layers at the TiO_2-terminated (001) surface of $BaTiO_3$ is illustrated in Fig. 1.

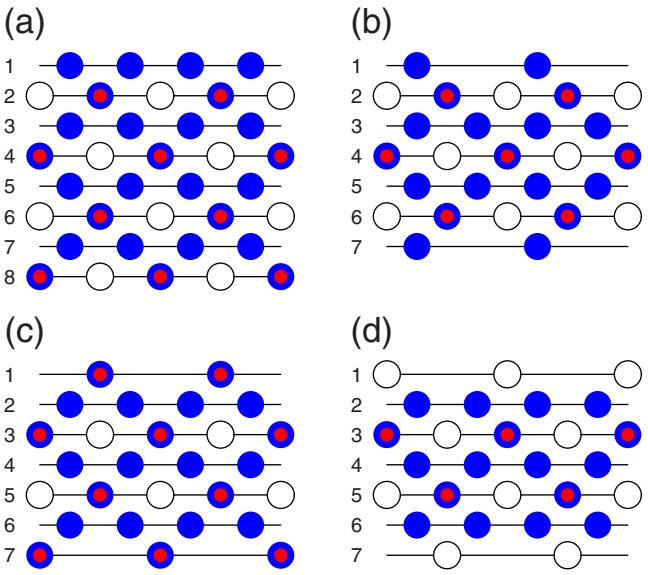

FIG. 2. (Color online) Side views of slab geometries used to study $BaTiO_3$ (011) surfaces. (a) Stoichiometric eight-layer slab with O_2-terminated and BaTiO-terminated surfaces at top and bottom, respectively. (b) Seven-layer slab with O-terminated surfaces. (c) Seven-layer slab with TiO-terminated surfaces. (d) Seven-layer slab with Ba-terminated surfaces.

Unlike the (001) cleavage of $BaTiO_3$ or $PbTiO_3$, which naturally gives rise to nonpolar BaO (or PbO) and TiO_2 terminations, a naive cleavage of $BaTiO_3$ or $PbTiO_3$ to create (011) surfaces leads to the formation of polar surfaces. For example, the stacking of the $BaTiO_3$ crystal along the (011) direction consists of alternating planes of O_2 and BaTiO units having nominal charges of $-4e$ and $+4e$, respectively, assuming O^{2-}, Ti^{4+}, and Ba^{2+} constituents. (Henceforth, we shall use $BaTiO_3$ for presentation purposes, but everything that is said will apply equally to the $PbTiO_3$ case.) Thus, a simple cleavage leads to O_2-terminated and BaTiO-terminated (011) surfaces that are *polar* and have nominal surface charges of $-2e$ and $+2e$ per surface cell, respectively. These are shown as the top and bottom surfaces in Fig. 2(a), respectively. If uncompensated, the surface charge would lead to an infinite electrostatic cleavage energy. In reality, the polar surfaces would probably become metallic in order to remain neutral, but in view of the large electronic gaps in the perovskites, such metallic surfaces would presumably be unfavorable. Thus, we may expect rather generally that such polar crystal terminations are relatively unstable in this class of materials.[3]

On the other hand, if the cleavage occurs in such a way as to leave a half layer of O_2 units on each surface, we obtain the nonpolar surface structure shown in Fig. 2(b). Every other surface O atom has been removed, and the remaining O atoms occupy the same sites as in the bulk structure. We shall refer to this as the "O-terminated" (011) surface, in distinction to the "O_2-terminated" polar surface already discussed in Fig. 2(a). The nonpolar nature of the O-terminated

TABLE I. Vertical atomic relaxations (in percent of bulk lattice constant) for $BaTiO_3$ and $PbTiO_3$ (001) surfaces. Positive sign corresponds to outward atomic displacement. "SM" indicates shell-model calculation of Ref. 16; "LDA" are previous calculations of Refs. 4 and 5 for $BaTiO_3$ and $PbTiO_3$, respectively.

$BaTiO_3$ (001) surface relaxations						$PbTiO_3$ (001) surface relaxations				
Termination	Layer	Ion	This study	SM	LDA	Termination	Layer	Ion	This study	LDA
BaO	1	Ba	−1.99	−3.72	−2.79	PbO	1	Pb	−3.82	−4.36
		O	−0.63	1.00	−1.40			O	−0.31	−0.46
	2	Ti	1.74	1.25	0.92		2	Ti	3.07	2.39
		O	1.40	0.76	0.48			O	2.30	1.21
	3	Ba		−0.51	0.53		3	Pb		−1.37
		O		0.16	0.26			O		−0.20
TiO_2	1	Ti	−3.08	−2.72	−3.89	TiO_2	1	Ti	−2.81	−3.40
		O	−0.35	−0.94	−1.63			O	0.31	−0.34
	2	Ba	2.51	2.19	1.31		2	Pb	5.32	4.53
		O	0.38	−0.17	−0.62			O	1.28	0.43
	3	Ti		−0.33	−0.75		3	Ti		−0.92
		O		−0.01	−0.35			O		−0.27

surface can be confirmed by noting that the 7-layer 15-atom $Ba_3Ti_3O_9$ slab shown in Fig. 2(b), which has two O-terminated surfaces, is neutral. It is also possible to make nonpolar TiO-terminated and Ba-terminated surfaces, as shown in Figs. 2(c) and 2(d), respectively. This is accomplished by splitting a BaTiO layer during cleavage, instead of splitting an O_2 layer. For the TiO- and Ba-terminated surfaces, we use seven-layer slabs having composition $Ba_2Ti_4O_{10}$ (16 atoms) and $Ba_4Ti_2O_8$ (14 atoms) as shown in Figs. 2(c) and 2(d), respectively. These are again neutral, showing that the surfaces are nonpolar (even though they no longer have precisely the bulk $BaTiO_3$ stoichiometry).

III. RESULTS OF CALCULATIONS

A. $BaTiO_3$ and $PbTiO_3$ (001) surface structures

In the present calculations of the $BaTiO_3$ and $PbTiO_3$ (001) surface atomic structures, we allowed the atoms located in the two outermost surface layers to relax along the z axis (the forces along the x and y axes are zero by symmetry). Here, we use the term "layer" to refer to a BaO, PbO, or TiO_2 plane, so that there are two layers per stacked unit cell. For example, on the BaO- or PbO-terminated surfaces, the top layer is BaO or PbO and the second layer is TiO_2; displacements of the third-layer atoms were found to be negligibly small in our calculations, and thus, were neglected.

The calculated atomic displacements for the TiO_2- and BaO-terminated (001) surfaces of $BaTiO_3$, and for the TiO_2- and PbO-terminated (001) surfaces of $PbTiO_3$, are presented in Table I. For $BaTiO_3$ (001), comparisons are also provided with the surface atomic displacements obtained by Padilla and Vanderbilt[4] using plane-wave DFT methods in the LDA, and by Heifets *et al.* using a classical SM approach.[16] Similarly, for $PbTiO_3$ (001), Table I shows comparisons with the plane-wave LDA calculations of Meyer *et al.*[5] The relaxation of the surface metal atoms in both the $BaTiO_3$ and $PbTiO_3$ surfaces is much larger than that of the oxygen ions, leading to a considerable surface rumpling, which we quantify via a parameter s defined as the relative displacement of the oxygen with respect to the metal atom in a given layer. The surface rumpling and relative displacements of three near-surface planes are presented in Table II. According to our calculations, atoms of the first surface layer relax inwards (i.e., toward the bulk) for BaO and PbO terminations of both materials. Our calculations are in qualitative agreement with the *ab initio* calculations performed by Padilla and Vanderbilt[4] for $BaTiO_3$, and by Meyer *et al.*[5] for $PbTiO_3$. However, the predictions of the SM calculation disagree with the first-principles calculations; the SM predicts that the first-layer oxygen ions relax outward on the BaO-terminated $BaTiO_3$ (001) surface,[16] rather than inwards. However, the magnitudes of the displacements are relatively small (−0.63% of the lattice constant a_0 in this study and 1.00% of a_0 in the SM calculations[16]), which may be close to the error bar of the classical shell model. Outward relaxations of all atoms in the second layer are found at both (001) terminations of the $BaTiO_3$ and $PbTiO_3$ surfaces. From Table I, we can conclude that the magnitudes of the atomic displacements calculated using different *ab initio* methods and using the classical shell model are in reasonable agreement.

In order to compare the calculated surface structures further with experimental results, the surface rumpling s and the changes in interlayer distances Δd_{12} and Δd_{23}, as defined in Fig. 1, are presented in Table II. Our calculations of the interlayer distances are based on the positions of relaxed metal ions, which are known to be much stronger electron scatterers than the oxygen ions.[19]

For $BaTiO_3$ (001), the rumpling of TiO_2-terminated surface is predicted to exceed that of BaO-terminated surface by a factor of 2. This finding is in line with the values of surface rumpling reported by Padilla and Vanderbilt.[4] In contrast, $PbTiO_3$ demonstrates practically the same rumpling for both terminations. From Table II, one can see that qualitative

TABLE II. Calculated surface rumpling s and interlayer displacements Δd_{ij} (in percent of bulk lattice constant) for near-surface planes on the BaO- or PbO- and TiO_2-terminated (001) surfaces of $BaTiO_3$ and $PbTiO_3$.

	BaO or PbO termination			TiO_2 termination		
	s	Δd_{12}	Δd_{23}	s	Δd_{12}	Δd_{23}
			$BaTiO_3$ (001)			
This study	1.37	−3.74	1.74	2.73	−5.59	2.51
LDA (Ref. 4)	1.39	−3.71	0.39	2.26	−5.20	2.06
SM (Ref. 16)	4.72	−4.97	1.76	1.78	−4.91	2.52
			$PbTiO_3$ (001)			
This study	3.51	−6.89	3.07	3.12	−8.13	5.32
LDA (Ref. 5)	3.9	−6.75	3.76	3.06	−7.93	5.45

agreement between all theoretical methods is obtained. In particular, the relaxed (001) surface structure shows a reduction of interlayer distance Δd_{12} and an expansion of Δd_{23} according to all *ab initio* and shell-model results.

As for experimental confirmation of these results, we are unfortunately unaware of experimental measurements of Δd_{12} and Δd_{23} for the $BaTiO_3$ and $PbTiO_3$ (001) surfaces. Moreover, for the case of the SrO-terminated $SrTiO_3$ (001) surface, existing LEED[19] and RHEED[20] experiments actually contradict each other regarding the sign of Δd_{12}. In view of the absence of clear experimental determinations of these parameters, therefore, the first-principles calculations are a particularly important tool for understanding the surface properties.

B. $BaTiO_3$ and $PbTiO_3$ (011) surface structures

We have performed *ab initio* calculations for $BaTiO_3$ and $PbTiO_3$ (011) surfaces. We have studied the TiO-terminated, Ba- or Pb-terminated, and O-terminated surfaces illustrated in Figs. 2(c), 2(d), and 2(b), respectively. The computed surface atomic relaxations are reported in Table III.

Focusing first on the $BaTiO_3$ surfaces, we find that the Ti ions in the outermost layer of the TiO-terminated surface move inwards (toward the bulk) by $0.0786a_0$, whereas the O ions in the outermost layer move outwards by $0.0261a_0$. The Ba atoms in the top layer of the Ba-terminated surface of Fig. 2(d) and the O atoms in the outermost layer of O-terminated surface of Fig. 2(b) move inwards by $0.0867a_0$ and $0.0540a_0$, respectively. The agreement between our *ab initio* B3PW and the classical SM calculations is satisfactory for all three of these surface terminations. In particular, the directions of the displacements of first- and second-layer atoms coincide for all three terminations. This indicates that classical SM calculations with a proper parametrization can serve as a useful initial approximation for modeling the atomic structure in perovskite thin films.

Turning now to our results for the $PbTiO_3$ (011) surfaces, we find that all metal atoms in the outermost layer move inwards irrespective of the termination. Surface oxygen atoms are displaced outwards for the TiO-terminated surface, while oxygen atoms move inwards in the O-terminated surface. The displacement patterns of atoms in the outermost surface layers are similar to those of the $BaTiO_3$ (011) surfaces, as well as classical shell-model results for $BaTiO_3$.[16] For example, the atomic displacement magnitudes of Ti and oxygen atoms in the TiO-terminated $PbTiO_3$ (011) surface are $-0.0813a_0$ and $0.033a_0$, respectively. The Pb atom is displaced inwards by $0.1194a_0$ for the Pb-terminated surface, similar to the corresponding $BaTiO_3$ case. Overall, Table III shows similar displacement patterns for the $BaTiO_3$ and $PbTiO_3$ (011) surfaces, as well as qualitatively similar results for both *ab initio* and classical shell-model descriptions.

C. $BaTiO_3$ and $PbTiO_3$ (001) and (011) surface energies

In the present work, we define the unrelaxed surface energy of a given surface termination X to be one-half of the energy needed to cleave the crystal rigidly into an unrelaxed surface X and an unrelaxed surface with the complementary termination X'. For $BaTiO_3$, for example, the unrelaxed surface energies of the complementary BaO- and TiO_2-terminated (001) surfaces are equal, as are those of the TiO- and Ba-terminated (011) surfaces (and similarly for $PbTiO_3$). The relaxed surface energy is defined to be the energy of the unrelaxed surface plus the (negative) surface relaxation energy. These definitions are chosen for consistency with Refs. 17 and 28. Unlike the authors of Refs. 27 and 29, we have made no effort to introduce chemical potentials here, so the results must be used with caution when addressing questions of the relative stability of surfaces with different stoichiometries.

With these definitions, and using the seven-layer slab geometries specified in Sec. II B, the energy of the unrelaxed $BaTiO_3$ (001) surface is

$$E_{\mathrm{surf}}^{\mathrm{unr}}(X) = \frac{1}{4}[E_{\mathrm{slab}}^{\mathrm{unr}}(\mathrm{BaO}) + E_{\mathrm{slab}}^{\mathrm{unr}}(\mathrm{TiO_2}) - 7E_{\mathrm{bulk}}], \qquad (1)$$

where X=BaO or TiO_2 specifies the termination, $E_{\mathrm{slab}}^{\mathrm{unr}}(\mathrm{BaO})$ and $E_{\mathrm{slab}}^{\mathrm{unr}}(\mathrm{TiO_2})$ are the unrelaxed BaO- and TiO_2-terminated slab energies, E_{bulk} is the energy per bulk $BaTiO_3$ unit cell, and the factor of 4 comes from the fact that four surfaces are

TABLE III. Calculated surface relaxations of $BaTiO_3$ and $PbTiO_3$ (011) surfaces (in percent of the lattice constant) for the three surface terminations. SM indicates comparative results from the shell-model calculation of Ref. 16.

$BaTiO_3$ (011) surface						$PbTiO_3$ (011) surface			
Layer	Ion	Δz	Δy	Δz (SM)	Δy (SM)	Layer	Ion	Δz	Δy
		TiO terminated					TiO terminated		
1	Ti	−7.86		−6.93		1	Ti	−8.13	
1	O	2.61		6.45		1	O	3.30	
2	O	−1.02		−1.66		2	O	−0.41	
3	Ba	−0.88		−3.85		3	Pb	−2.54	
3	O			−2.40		3	O	−4.07	
3	Ti			1.59		3	Ti	0.30	
		Ba terminated					Pb terminated		
1	Ba	−8.67		−13.49		1	Pb	−11.94	
2	O	0.80		2.80		2	O	−0.61	
3	Ti	0.16		−1.20		3	Ti	1.78	
3	O	−0.43		−2.94		3	O	1.67	
3	Ba			2.52		3	Pb	1.52	
		O terminated					O terminated		
1	O	−5.40	−1.67	−11.16	−6.70	1	O	−7.37	−0.07
2	Ti	−0.15	−6.38	−1.83	−5.33	2	Ti	0.20	−2.54
2	Ba	1.54	−1.27	4.84	−2.21	2	Pb	0.18	−7.50
2	O	1.95	2.97	4.54	5.90	2	O	0.51	2.19
3	O	0.90	4.49	6.52	5.58	3	O	−0.41	3.30

created by the two cleavages needed to make the two slabs. The relaxation energy for each termination can be computed from the corresponding slab alone using

$$\Delta E_{\mathrm{surf}}^{\mathrm{rel}}(X) = \frac{1}{2}[E_{\mathrm{slab}}(X) - E_{\mathrm{slab}}^{\mathrm{unr}}(X)], \tag{2}$$

where $E_{\mathrm{slab}}(X)$ is a slab energy after relaxation. The relaxed surface energy is then

$$E_{\mathrm{surf}}(X) = E_{\mathrm{surf}}^{\mathrm{unr}}(X) + \Delta E_{\mathrm{surf}}^{\mathrm{rel}}(X). \tag{3}$$

Similarly, for the $BaTiO_3$ (011) case, a cleavage on a bulk BaTiO plane gives rise to the complementary TiO- and Ba-terminated surfaces shown in Figs. 2(c) and 2(d), respectively. Thus,

$$E_{\mathrm{surf}}^{\mathrm{unr}}(X) = \frac{1}{4}[E_{\mathrm{slab}}^{\mathrm{unr}}(\mathrm{Ba}) + E_{\mathrm{slab}}^{\mathrm{unr}}(\mathrm{TiO}) - 6E_{\mathrm{bulk}}], \tag{4}$$

where the energy is the same for X=TiO or Ba, $E_{\mathrm{slab}}^{\mathrm{unrel}}(\mathrm{Ba})$ and $E_{\mathrm{slab}}^{\mathrm{unrel}}(\mathrm{TiO})$ are energies of the unrelaxed slabs. Relaxation energies can again be computed independently for each slab in a manner similar to Eq. (2). Finally, the (011) surface can also be cleaved to give two identical self-complementary O-terminated surfaces of the kind shown in Fig. 2(b).

In this case, the seven-layer slab has the stoichiometry of three bulk unit cells, so the relaxed surface energy of the O-terminated (011) surface is

$$E_{\mathrm{surf}}(O) = \frac{1}{2}[E_{\mathrm{slab}}(O) - 3E_{\mathrm{bulk}}], \tag{5}$$

where $E_{\mathrm{slab}}(O)$ is the relaxed energy of the slab having two O-terminated surfaces. Everything said here about $BaTiO_3$ surfaces applies in exactly the same way to the corresponding $PbTiO_3$ surfaces.

The calculated surface energies of the relaxed $BaTiO_3$ (001) and (011) surfaces are presented in Table IV. In $BaTiO_3$, the relaxation energies of the TiO_2- and BaO-terminated surfaces (−0.23 and −0.11 eV, respectively) are comparable, leading to rather similar surface energies. On the (011) surfaces, however, the relaxation energies vary more strongly with termination. For example, we find a relaxation energy of −2.13 eV for the TiO-terminated surface, much larger than −0.93 eV for the Ba-terminated surface. The relaxation energy of −1.15 eV for O-terminated surface gives rise to a relaxed energy of the O-terminated surface (1.72 eV) that is much lower than the average of the TiO- and Ba-terminated surfaces (2.64 eV), indicating that it takes much less energy to cleave on an O_2 plane than on a BaTiO plane. The shell-model results of Ref. 16 for the $BaTiO_3$ surfaces are shown for comparison; the results are qualitatively similar, but there are some significant quantitative differences, especially for the Ba-terminated (011) surface.

The corresponding results are also given for the (001) and (011) surfaces of $PbTiO_3$ in Table IV. The results for the

TABLE IV. Calculated surface energies for $BaTiO_3$ and $PbTiO_3$ (001) and (011) surfaces (in eV per surface cell). SM indicates comparative results from the shell-model calculation of Ref. 16.

Surface	Termination	E_{surf}	E_{surf} (SM)
$BaTiO_3$ (001)	TiO_2	1.07	1.40
	BaO	1.19	1.45
$BaTiO_3$ (011)	TiO	2.04	2.35
	Ba	3.24	4.14
	O	1.72	1.81
$PbTiO_3$ (001)	TiO_2	0.74	
	PbO	0.83	
$PbTiO_3$ (011)	TiO	1.36	
	Pb	2.03	
	O	1.72	

(001) surfaces are similar to those for $BaTiO_3$, although the relaxed surface energies are somewhat lower. For the case of the (011) surfaces, however, we find a different pattern than for $BaTiO_3$. We find a very large relaxation energy of −1.75 eV for the TiO-terminated surface, compared with −1.08 eV for the Pb-terminated surface and −1.12 eV for the O-terminated surface. The average energy of the TiO- and Pb-terminated surfaces is now 1.69 eV, compared with 1.72 eV for the O-terminated surface, indicating that the cleavage on a PbTiO or an O_2 plane has almost exactly the same energy cost.

D. $BaTiO_3$ and $PbTiO_3$ (001) and (011) surface charge distributions and chemical bondings

To characterize the chemical bonding and covalency effects, we used a standard Mulliken population analysis for the effective static atomic charges Q and other local properties of the electronic structure as described, for example, in Refs. 39 and 40. The results are presented in Table V. Our calculated effective charges for bulk $PbTiO_3$ are $+1.354e$ for the Pb atom, $+2.341e$ for the Ti atom, and $-1.232e$ for the O atom. The bond population describing the chemical bonding is $+98me$ between Ti and O atoms, $+16me$ between Pb and O atoms, and $+2me$ between Pb and Ti atoms. Our calculated effective charges for bulk $BaTiO_3$ are $+1.797e$ for the Ba atom, $+2.367e$ for the Ti atom, and $-1.388e$ for the O atom, indicating a high degree of $BaTiO_3$ chemical bond covalency. The bond population between Ti and O atoms in $BaTiO_3$ bulk is exactly the same as in $PbTiO_3$, while that between Ba and Ti is slightly negative, suggesting a repulsive interaction between these atoms in the bulk of the $BaTiO_3$ crystal.

TABLE V. Calculated magnitudes of atomic displacements D (in Å), effective atomic charges Q (in e), and bond populations P between metal-oxygen nearest neighbors (in $10^{-3}e$) for the $BaTiO_3$ and $PbTiO_3$ (001) surfaces.

		$BaTiO_3$ (001) surface				$PbTiO_3$ (001) surface			
Layer	Property	Ion	TiO_2 terminated	Ion	BaO terminated	Ion	TiO_2 terminated	Ion	PbO terminated
1	D	Ti	−0.123	Ba	−0.080	Ti	−0.111	Pb	−0.150
	Q		2.307		1.752		2.279		1.276
	P		126		−30		114		54
	D	O	−0.014	O	−0.025	O	0.012	O	−0.012
	Q		−1.280		−1.473		−1.184		−1.128
	P		−38		80		44		106
2	D	Ba	0.101	Ti	0.070	Pb	0.209	Ti	0.121
	Q		1.767		2.379		1.275		2.331
	P		−30		88		8		80
	D	O	0.015	O	0.056	O	0.050	O	0.091
	Q		−1.343		−1.418		−1.167		−1.258
	P		90		−30		80		6
3	Q	Ti	2.365	Ba	1.803	Ti	2.335	Pb	1.358
	P		104		−36		108		24
	Q	O	−1.371	O	−1.417	O	−1.207	O	−1.259
	P		−34		98		18		96
Bulk	Q	Ba	1.797	Ba	1.797	Pb	1.354	Pb	1.354
	P		−34		−34		16		16
	Q	O	−1.388	O	−1.388	O	−1.232	O	−1.232
	P		98		98		98		98
	Q	Ti	2.367	Ti	2.367	Ti	2.341	Ti	2.341

TABLE VI. The $A-B$ bond populations P (in $10^{-3}e$) and interatomic distances R (in Å) on (011) surfaces of $BaTiO_3$ and $PbTiO_3$. Symbols I–IV denote the number of each plane enumerated from the surface. The nearest-neighbor Ti-O distance is 2.004 and 1.968 Å in bulk $BaTiO_3$ and $PbTiO_3$, respectively.

$BaTiO_3$ (011) surface				$PbTiO_3$ (011) surface			
Atom A	Atom B	P	R	Atom A	Atom B	P	R
	TiO terminated				TiO terminated		
Ti(I)	O(I)	130	2.047	Ti(I)	O(I)	132	2.019
	O(II)	198	1.784		O(II)	196	1.766
O(II)	Ti(III)	112	2.009	O(II)	Ti(III)	120	1.948
	Ba(III)	−24	2.808		Pb(III)	24	2.826
	O(III)	−26	2.837		O(III)	−20	2.857
Ti(III)	Ba(III)	−2	3.471	Ti(III)	Pb(III)	2	3.410
	O(III)	118	2.004		O(III)	108	1.975
	O(IV)	96	2.004		O(IV)	88	1.976
Ba(III)	O(III)	−32	2.834	Pb(III)	O(III)	20	2.783
	O(IV)	−38	2.816		O(IV)	8	2.734
O(III)	O(IV)	−30	2.834	O(III)	O(IV)	−36	2.706
	Ba terminated				Pb terminated		
Ba(I)	O(II)	−38	2.664	Pb(I)	O(II)	126	2.589
O(II)	Ba(III)	−36	2.850	O(II)	Pb(III)	24	2.742
	Ti(III)	84	2.022		Ti(III)	74	1.902
	O(III)	−38	2.859		O(III)	−46	2.739
Ba(III)	O(III)	−36	2.834	Pb(III)	O(III)	−10	2.783
	O(IV)	−36	2.834		O(IV)	36	2.813
Ti(III)	O(III)	76	2.004	Ti(III)	O(III)	62	1.968
	Ba(III)	−2	3.471		Pb(III)	0	3.408
	O(IV)	98	2.008		O(IV)	92	2.018
O(III)	O(IV)	−46	2.825	O(III)	O(IV)	−46	2.816
	O terminated				O terminated		
O(I)	Ba(II)	−26	2.697	O(I)	Pb(II)	50	2.503
	Ti(II)	168	1.722		Ti(II)	128	1.694
	O(II)	−24	2.801		O(II)	−26	2.689
Ba(II)	O(II)	−40	2.664	Pb(II)	O(II)	78	2.574
	Ti(II)	−2	3.306		Ti(II)	4	3.094
Ti(II)	O(II)	82	2.040	Ti(II)	O(II)	92	1.977
	O(III)	112	1.689		O(III)	126	1.831
O(II)	O(III)	−12	2.825	O(II)	O(III)	−24	2.779
Ba(II)	O(III)	−10	2.968	Pb(II)	O(III)	26	2.716
O(III)	O(IV)	−14	2.945	O(III)	O(IV)	−42	2.842
	Ti(IV)	60	2.159		Ti(IV)	60	2.051
	Ba(IV)	−24	2.767		Pb(IV)	−2	2.712

For the TiO_2-terminated $BaTiO_3$ and $PbTiO_3$ (001) surfaces, the major effect observed here is a strengthening of the Ti-O chemical bond near the $BaTiO_3$ and $PbTiO_3$ (001) surfaces, which was already pronounced for both materials in the bulk. Note that the Ti and O effective charges for bulk $BaTiO_3$ and $PbTiO_3$ are much smaller than those expected in an ionic model ($+4e$ and $-2e$), and that the Ti-O chemical bonds in bulk $BaTiO_3$ and $PbTiO_3$ are fairly heavily populated for both materials.

The Ti-O bond populations for the TiO_2-terminated $BaTiO_3$ and $PbTiO_3$ (001) surfaces are $+126me$ and $+114me$, respectively, which are about 20% larger than the relevant value in the bulk. In contrast, the Pb-O bond population of $+54me$ is small for the PbO-terminated $PbTiO_3$ (001) surface, and the Ba-O bond population of $-30me$ is even negative for the BaO-terminated $BaTiO_3$ (001) surface, indicating a repulsive character. The effect of the difference in the chemical bonding is also well seen from the Pb and Ba

effective charges in the first surface layer, which are close to the formal ionic charge of $+2e$ only in the case of the $BaTiO_3$ crystal.

The interatomic bond populations for three possible $BaTiO_3$ and $PbTiO_3$ (011) surface terminations are given in Table VI. The major effect observed here is a strong increase of the Ti-O chemical bonding near the $BaTiO_3$ and $PbTiO_3$ (011) surfaces as compared to the already large bonding near the (001) surfaces (+126me and +114me, respectively) and in the bulk (+98me). For the O-terminated (011) surface, the O(I)-Ti(II) bond population is as large as +168me for $BaTiO_3$ and +128me for $PbTiO_3$, i.e., considerably larger than in the bulk and on the (001) surface.

Our calculations demonstrate that for the TiO-terminated $BaTiO_3$ and $PbTiO_3$ (011) surfaces, the Ti-O bond populations are larger in the direction perpendicular to the surface (+198me for $BaTiO_3$ and +196me for $PbTiO_3$) than in plane (+130me for $BaTiO_3$ and +132me for $PbTiO_3$). The Ti-O bond populations for the TiO-terminated $PbTiO_3$ (011) surface in the direction perpendicular to the surface are twice as large as the Ti-O bond population in $PbTiO_3$ bulk.

In Table VII, we present the calculated Mulliken effective charges Q, and their changes ΔQ with respect to the bulk values, near the surface. We analyzed the charge redistribution between different layers in slabs with all three $BaTiO_3$ and $PbTiO_3$ (011) surface terminations. The charge of the surface Ti atoms in the TiO-terminated $BaTiO_3$ and $PbTiO_3$ (001) surfaces is reduced by $0.151e$ and $0.129e$, respectively. Metal atoms in the third layer lose much less charge. Except in the central layer (and, in the case of $PbTiO_3$, in the subsurface layer), the O ions also reduce their charges, becoming less negative. The largest charge change is observed for $BaTiO_3$ and $PbTiO_3$ subsurface O atoms ($+0.233e$ and $+0.175e$, respectively). This gives a large positive change of $+0.466e$ and $+0.350e$ in the charge for each $BaTiO_3$ and $PbTiO_3$ subsurface layer.

On the Ba-terminated and Pb-terminated $BaTiO_3$ and $PbTiO_3$ (011) surfaces, negative changes in the charge are observed for all atoms except for Ba and Ti in the $BaTiO_3$ third layer, Ti atom in the $PbTiO_3$ third layer, and subsurface oxygen atom in $PbTiO_3$. The largest charge changes are at the surface Ba and Pb ions. It is interesting to notice that, due to the tiny difference in the chemical bonding between $BaTiO_3$ and $PbTiO_3$ perovskites, the charge changes for the

TABLE VII. Calculated Mulliken atomic charges Q (in e) and changes in atomic charges ΔQ with respect to the bulk charges (in e) on (011) surfaces of $BaTiO_3$ and $PbTiO_3$, for three terminations. The Mulliken charges are $2.341e$ for Ti, $-1.232e$ for O, and $1.354e$ for Pb in bulk $PbTiO_3$, and $2.367e$ for Ti, $-1.388e$ for O, and $1.797e$ for Ba in bulk $BaTiO_3$.

$BaTiO_3$ (011) surface			$PbTiO_3$ (011) surface		
Atom	Q	ΔQ	Atom	Q	ΔQ
	TiO terminated			TiO terminated	
Ti(I)	2.216	−0.151	Ti(I)	2.212	−0.129
O(I)	−1.316	0.072	O(I)	−1.261	−0.029
O(II)	−1.155	0.233	O(II)	−1.057	0.175
Ba(III)	1.757	−0.04	Pb(III)	1.253	−0.101
Ti(III)	2.353	−0.014	Ti(III)	2.328	−0.013
O(III)	−1.299	0.089	O(III)	−1.18	0.052
O(IV)	−1.402	−0.014	O(IV)	−1.239	−0.007
	Ba terminated			Pb terminated	
Ba(I)	1.636	−0.161	Pb(I)	1.122	−0.232
O(II)	−1.483	−0.095	O(II)	−1.140	0.092
Ba(III)	1.799	0.002	Pb(III)	1.340	−0.014
Ti(III)	2.368	0.001	Ti(III)	2.343	0.002
O(III)	−1.446	−0.058	O(III)	−1.277	−0.045
O(IV)	−1.392	−0.004	O(IV)	−1.247	−0.015
	O terminated			O terminated	
O(I)	−1.158	0.23	O(I)	−1.011	0.221
Ba(II)	1.766	−0.031	Pb(II)	1.257	−0.097
Ti(II)	2.213	−0.154	Ti(II)	2.237	−0.104
O(II)	−1.452	−0.064	O(II)	−1.261	−0.029
O(III)	−1.317	0.071	O(III)	−1.215	0.017
Ba(IV)	1.792	−0.005	Pb(IV)	1.355	0.001
Ti(IV)	2.317	−0.05	Ti(IV)	2.317	−0.024
O(IV)	−1.407	−0.019	O(IV)	−1.233	−0.001

$BaTiO_3$ subsurface O ion ($-0.095e$) and $PbTiO_3$ subsurface O ion ($+0.092e$) have practically the same magnitude, but opposite signs.

For the O-terminated $BaTiO_3$ and $PbTiO_3$ (011) surfaces, the largest calculated changes in the charge are observed for the $BaTiO_3$ and $PbTiO_3$ surface O atoms ($+0.230e$ and $+0.221e$, respectively). The change of the total charge in the second layer is negative and almost equal for both materials. For the $BaTiO_3$ crystal, this reduction by $0.249e$ comes mostly from the Ti atom ($-0.154e$). In the $PbTiO_3$ crystal, the reduction by $0.230e$ appears mostly due to a decrease of the Ti atom charge by $0.104e$ as well as a reduction of the Pb atom charge by $0.097e$.

IV. CONCLUSIONS

In summary, motivated by the scarcity of experimental investigations of the $BaTiO_3$ and $PbTiO_3$ surfaces and the contradictory experimental results obtained for the related $SrTiO_3$ surface,[19,20] we have carried out a predictive electronic structure calculation to investigate the surface atomic and electronic structures of the $BaTiO_3$ and $PbTiO_3$ (001) and (011) surfaces. Using a hybrid B3PW approach, we have calculated the surface relaxation of the two possible terminations (TiO_2 and BaO or PbO) of the $BaTiO_3$ and $PbTiO_3$ (001) surfaces, and three possible terminations (TiO, Ba or Pb, and O) of the $BaTiO_3$ and $PbTiO_3$ (011) surfaces. The data obtained for the surface structures are in good agreement with previous LDA calculations of Padilla and Vanderbilt[4] the LDA plane-wave calculations of Meyer *et al.*,[5] and in fair agreement with the shell-model calculations of Heifets *et al.*[16]

According to our calculations, atoms of the first surface layer relax inwards for BaO- and PbO-terminated (001) surfaces of both materials. Outward relaxations of all atoms in the second layer are found at both terminations of $BaTiO_3$ and $PbTiO_3$ (001) surfaces. In $BaTiO_3$, the rumpling of the TiO_2-terminated (001) surface is predicted to exceed that of the BaO-terminated (001) surface by a factor of 2. In contrast, $PbTiO_3$ exhibits practically the same rumplings for both (TiO_2 and PbO) terminations. Our calculated surface energies show that the TiO_2-terminated (001) surface is slightly more stable for both materials than the BaO- or PbO-terminated (001) surface. The O-terminated $BaTiO_3$ and TiO-terminated $PbTiO_3$ (011) surfaces have surface energies close to that of the (001) surface. Our calculations suggest that the most unfavorable (011) surfaces are the Ba- or Pb-terminated ones for both the $BaTiO_3$ and $PbTiO_3$ cases. We found that the relaxation of the $BaTiO_3$ and $PbTiO_3$ surfaces is considerably stronger for all three (011) terminations than for the (001) surfaces. The atomic displacements in the third plane from the surface for the three terminations of $BaTiO_3$ and $PbTiO_3$ (011) surfaces are still large. Finally, our *ab initio* calculations indicate a considerable increase of Ti-O bond covalency near the $BaTiO_3$ and $PbTiO_3$ (011) surfaces relative to $BaTiO_3$ and $PbTiO_3$ bulk, much larger than for the (001) surface.

ACKNOWLEDGMENTS

The present work was supported by Deutsche Forschungsgemeinschaft (DFG) and by ONR Grant No. N00014-05-1-0054.

[1] J. F. Scott, *Ferroelectric Memories* (Springer, Berlin, 2000).
[2] M. E. Lines and A. M. Glass, *Principles and Applications of Ferroelectrics and Related Materials* (Clarendon, Oxford, 1977).
[3] C. Noguera, *Physics and Chemistry at Oxide Surfaces* (Cambridge University Press, New York, 1996).
[4] J. Padilla and D. Vanderbilt, Phys. Rev. B **56**, 1625 (1997).
[5] B. Meyer, J. Padilla, and D. Vanderbilt, Faraday Discuss. **114**, 395 (1999).
[6] F. Cora and C. R. A. Catlow, Faraday Discuss. **114**, 421 (1999).
[7] L. Fu, E. Yaschenko, L. Resca, and R. Resta, Phys. Rev. B **60**, 2697 (1999).
[8] C. Cheng, K. Kunc, and M. H. Lee, Phys. Rev. B **62**, 10409 (2000).
[9] B. Meyer and D. Vanderbilt, Phys. Rev. B **63**, 205426 (2001).
[10] C. Bungaro and K. M. Rabe, Phys. Rev. B **71**, 035420 (2005).
[11] M. Krcmar and C. L. Fu, Phys. Rev. B **68**, 115404 (2003).
[12] Y. Umeno, T. Shimada, T. Kitamura, and C. Elsasser, Phys. Rev. B **74**, 174111 (2006).
[13] B. K. Lai, I. Ponomareva, I. A. Kornev, L. Bellaiche, and G. J. Salamo, Phys. Rev. B **75**, 085412 (2007).
[14] E. Heifets, S. Dorfman, D. Fuks, E. Kotomin, and A. Gordon, J. Phys.: Condens. Matter **10**, L347 (1998).
[15] S. Tinte and M. G. Stachiotti, in *Fundamental Physics of Ferroelectrics 2000*, edited by Ronald E. Cohen, AIP Conf. Proc. No. 535 (AIP, Melville, NY, 2000), p. 273.
[16] E. Heifets, E. Kotomin, and J. Maier, Surf. Sci. **462**, 19 (2000).
[17] E. Heifets, R. I. Eglitis, E. A. Kotomin, J. Maier, and G. Borstel, Phys. Rev. B **64**, 235417 (2001).
[18] E. Heifets, R. I. Eglitis, E. A. Kotomin, J. Maier, and G. Borstel, Surf. Sci. **513**, 211 (2002).
[19] N. Bickel, G. Schmidt, K. Heinz, and K. Muller, Phys. Rev. Lett. **62**, 2009 (1989).
[20] T. Hikita, T. Hanada, M. Kudo, and M. Kawai, Surf. Sci. **287-288**, 377 (1993).
[21] A. Ikeda, T. Nishimura, T. Morishita, and Y. Kido, Surf. Sci. **433-435**, 520 (1999).
[22] G. Charlton, S. Brennan, C. A. Muryn, R. McGrath, D. Norman, T. S. Turner, and G. Thorthon, Surf. Sci. **457**, L376 (2000).
[23] P. A. W. van der Heide, Q. D. Jiang, Y. S. Kim, and J. W. Rabalais, Surf. Sci. **473**, 59 (2001).
[24] W. Maus-Friedrichs, M. Frerichs, A. Gunhold, S. Krischok, V. Kempter, and G. Bihlmayer, Surf. Sci. **515**, 499 (2002).
[25] K. Szot and W. Speier, Phys. Rev. B **60**, 5909 (1999).
[26] J. Brunen and J. Zegenhagen, Surf. Sci. **389**, 349 (1997).
[27] F. Bottin, F. Finocchi, and C. Noguera, Phys. Rev. B **68**, 035418

(2003).
[28] E. Heifets, W. A. Goddard III, E. A. Kotomin, R. I. Eglitis, and G. Borstel, Phys. Rev. B **69**, 035408 (2004).
[29] E. Heifets, J. Ho, and B. Merinov, Phys. Rev. B **75**, 155431 (2007).
[30] V. R. Saunders, R. Dovesi, C. Roetti, M. Causa, N. M. Harrison, R. Orlando, and C. M. Zicovich-Wilson, *CRYSTAL2003 Users Manual* (University of Torino, Torino, 2003).
[31] R. E. Cohen, J. Phys. Chem. Solids **57**, 1393 (1996).
[32] R. E. Cohen, Ferroelectrics **194**, 323 (1997).
[33] S. Piskunov, E. Heifets, R. I. Eglitis, and G. Borstel, Comput. Mater. Sci. **29**, 165 (2004).
[34] A. D. Becke, J. Chem. Phys. **98**, 5648 (1993).
[35] J. P. Perdew and Y. Wang, Phys. Rev. B **33**, 8800 (1986).
[36] J. P. Perdew and Y. Wang, Phys. Rev. B **40**, 3399 (1989).
[37] J. P. Perdew and Y. Wang, Phys. Rev. B **45**, 13244 (1992).
[38] H. J. Monkhorst and J. D. Pack, Phys. Rev. B **13**, 5188 (1976).
[39] C. R. A. Catlow and A. M. Stoneham, J. Phys. C **16**, 4321 (1983).
[40] R. C. Bochiccio and H. F. Reale, J. Phys. B **26**, 4871 (1993).